

¹⁸F-DCFPyL PET/CT in Patients with Subclinical Recurrence of Prostate Cancer: Effect of Lesion Size, Smooth Filter and Partial Volume Correction on Prostate Cancer Molecular Imaging Standardized Evaluation (PROMISE) criteria

Claudia Ortega^{1*}, Josh Schaefferkoetter^{1,2*}, Patrick Veit-Haibach¹, Reut Anconina¹, Alejandro Berlin³, Nathan Perlis⁴, Ur Metser¹

**Equally contributed to this work*

¹ Joint Department of Medical Imaging, Princess Margaret Hospital, University Health Network, Mount Sinai Hospital and Women's College Hospital, University of Toronto, 610 University Ave, Toronto, ON, Canada M5G 2M9.

² Siemens Healthcare Limited, Oakville, ON, Canada.

³ Radiation Medicine Program, Princess Margaret Hospital, University Health Network, Toronto, ON, Canada.

⁴ Urologic Oncology, University Health Network, Princess Margaret Cancer Centre Research Institute, University of Toronto, Toronto, ON, Canada.

Corresponding author:

Ur Metser, MD, FRCPC

Professor, Department of Medical Imaging, University of Toronto

Joint Department of Medical Imaging

610 University Ave, Suite 3-960 Toronto, ON, Canada M5G 2M9

Email - Ur.metser@uhn.ca

Phone: 416-946 4501 ext 4394; Fax: 416-946 6564

<https://orcid.org/0000-0003-3726-8994>

First authors:

Claudia Ortega, MD

Joint Department of Medical Imaging

610 University Ave, Suite 3-960 Toronto, ON, Canada M5G 2M9

Email – Claudia.Ortega@uhn.ca

Phone: 416-946 4501 ext 4394; Fax: 416-946 6564

Josh Schaefferkoetter, PhD

Siemens Healthcare Limited, Oakville, ON, Canada.

Email: jschaefferkoetter@gmail.com

Phone: 647-746 4462

Running title: Partial volume effect on PSMA uptake

ABSTRACT

Purpose To determine the effect of smooth filter and partial volume correction (PVC) method on measured prostate-specific membrane antigen (PSMA) activity in small metastatic lesions and to determine the impact of these changes on the molecular imaging (mi) PSMA scoring. **Materials & Methods** Men with biochemical recurrence of prostate cancer with negative CT and bone scintigraphy were referred for ^{18}F -DCFPyL PET/CT. Examinations were performed on one of 2 PET/CT scanners (GE Discovery 610 or Siemens mCT40). All suspected tumor sites were manually contoured on co-registered CT and PET images, and each was assigned a miPSMA score as per the PROMISE criteria. The PVC factors were calculated for every lesion using the anatomical CT and then applied to the unsmoothed PET images. The miPSMA scores, with and without the corrections, were compared, and a simplified “rule of thumb” (RoT) correction factor (CF) was derived for lesions at various sizes (<4mm, 4-7mm, 7-9mm, 9-12mm). This was then applied to the original dataset and miPSMA scores obtained using the RoT CF were compared to those found using the actual corrections. **Results** There were 75 men (median age, 69 years; median serum PSA of 3.69 ug/L) with 232 metastatic nodes < 12 mm in diameter (mean lesion volume of $313.5 \pm 309.6 \text{ mm}^3$). Mean SUVmax before and after correction was 11.0 ± 9.3 and 28.5 ± 22.8 , respectively ($p < 0.00001$). The mean CF for lesions <4mm (n=22), 4-7mm (n=140), 7-9mm (n=50), 9-12 mm (n=20) was 4 (range: 2.5-6.4), 2.8 (range: 1.6-4.9), 2.3 (range: 1.6-3.3) and 1.8 (range 1.4-2.4), respectively. Overall miPSMA scores were concordant between the corrected dataset and RoT in 205/232 lesions (88.4%). **Conclusion** There is a significant effect of smooth filter and partial volume correction on measured PSMA activity in small nodal metastases, impacting the miPSMA score.

INTRODUCTION

Prostate-specific membrane antigen (PSMA) PET imaging offers unparalleled accuracy in assessment of patients with prostate cancer. The main evaluated clinical indications to date for PSMA PET are for restaging of patients with prostate cancer after primary therapy with biochemical failure, or for the initial staging of high risk or unfavorable intermediate risk prostate cancer (1). Various PSMA tracers are available. The most widely used PSMA radiotracer is ^{68}Ga -PSMA-11 (also named ^{68}Ga -PSMA-HBED-CC). Recently introduced ^{18}F -labelled PSMA tracers have the advantage of cyclotron production, enabling multiple doses from a single formulation, longer half-life of ^{18}F compared to ^{68}Ga , facilitating shipping of the tracer to off-site facilities, lower energy and shorter positron range, allowing for higher image resolution (2). One such tracer is ^{18}F -DCFPyL(2-(3-(1-carboxy-5-[(6- ^{18}F -fluoro-pyridine-3-carbonyl)-amino]-pentyl),a promising second generation low molecular weight ligand (3).

Recently, the *Prostate Cancer Molecular Imaging Standardized Evaluation* (PROMISE) criteria were introduced to standardize the interpretation of PSMA PET (4). PROMISE suggests a molecular imaging TNM system (miTNM, version 1.0). In this staging algorithm, each suspected primary or recurrent tumor (T), regional nodal metastasis (N) and distant metastasis (M1a-M1c) are assigned a diagnosis of positive, negative or equivocal depending on the degree of PSMA expression and findings on morphological imaging (CT or MRI). PSMA PET uptake at suspected tumor sites is quantified using a PSMA scoring system relative to the physiological uptake in reference tissues with the parotid gland, liver, and blood pool activity serving as the reference for high, intermediate and low level PSMA uptake, respectively [Table 1].

For accurate quantification of radiotracer uptake on PET, several corrections are needed such as taking partial volume effect (PVE) into account (5). PVE originates from the finite spatial resolution of the PET scanner and causes underestimation of the measured activity concentration especially for lesions at or below the resolution of the scanner (6). Partial volume effects in medical imaging result from the combination of limited scanner resolution and heterogeneous tissue types within voxels of finite dimensions. Accurate quantification of metabolic volumes when they are below 2 or 3 times the spatial resolution of the PET scanner are hampered by partial volume effects, leading to underestimation of SUV or even under-detection of small lesions (7). Furthermore, PET images are affected by routinely applied Gaussian filters. These effects degrade resolution and quantitative accuracy and are especially problematic for PET imaging due to its relatively coarse pixel sizes.

These two factors, smooth filter and partial volume correction may play a significant role in the measured individual lesion activity, particularly for small volume tumor foci. These are increasingly common as PSMA PET is adopted for the management of prostate cancer, especially in patients with subclinical recurrent or metastatic disease, with no gross detectable metastatic disease on CT and bone scintigraphy. In these patients, accurate identification of all disease sites may have significant clinical implications to tailoring the most appropriate therapeutic approach. The aim of the current study was to determine and quantify the effect of smooth filter and Partial Volume Correction (PVC) method on measured PSMA activity in small metastatic lesions (e.g. <12mm) and to ascertain their impact on the miPSMA scoring.

MATERIALS AND METHODS

Patient Population

The cohort for this study included patients from 2 prospective institutional ethics review board approved clinical trials from May 2018 to February 2019 (NCT03718260 and NCT03160794). Written informed consent was obtained from all subjects. In both of these trials, subjects had biochemical recurrence after primary therapy with subclinical metastases defined as asymptomatic recurrence with negative or equivocal conventional workup (bone scintigraphy and CT). CT and bone scintigraphy were interpreted clinically prior to study accrual. Patients underwent ^{18}F -DCFPyL PET/CT between May 2018 and February 2019.

^{18}F -DCFPyL PET Imaging

^{18}F -DCFPyL was synthesized as previously described (8). PET was performed on one of 2 scanners (Siemens mCT40, Siemens Healthcare, Erlangen, Germany; or General Electric Discovery 610, GE Healthcare, Waukesha, WI). Approximately 120 minutes (mean, 115.1 min; range: 83-168) after intravenous injection of 335.5 MBq (range: 223-376) of ^{18}F -DCFPyL, a second generation low-molecular weight PSMA PET radiotracer. Patients were asked to void bladder and subsequently positioned supine on the imaging couch with arms outside of the region of interest. Images were obtained from the top of the skull to the upper thighs. Iodinated oral contrast material was administered for bowel opacification; no intravenous iodinated contrast was used. The acquisition time was 8 min per bed position for the pelvis and 2 min per bed position for all other bed positions. Overall, 5-9 bed positions were obtained as per patient height. The technical parameters for the 2 PET scanners were as follows: 1. Siemens mCT40 (Siemens Healthcare). CT parameters were 120 kV; 5.0 mm slice width, 4.0 mm collimation; 0.8 sec rotation time; 8.4 mm feed/rotation; Kernel B30s medium smooth reconstruction. PET

emission scan using time of flight (TOF) with scattered correction was obtained covering the identical transverse field of view. Image size: 2.6 pix size; slice 3.27; 5mm FWHM Gaussian Filter type; 31/21s iterations/subsets. 2. General Electric Discovery 610 scanner (GE Healthcare). CT parameters are 120 kV; 150 – 190 mA depending of weight; 3.75 mm helical thickness, 0.8 sec rotation time, 11.25 mm feed/rotation; Standard reconstruction at 2.5 mm thickness. PET parameters are: 3.18 pixel size; 6.4 mm filter FWHM, Gaussian Filter with 2i/32s iterations/subsets. Scan parameters were the clinical standard at each site and were selected according to vendor recommendations for each scanner.

Image Analysis

All suspected tumor foci on ^{18}F -DCFPyL PET/CT were manually contoured on the non-contrast CT (acquired at time of PET/CT) and independently on the 5 mm Gaussian-smoothed PET, using a Mirada Vision workstation (Mirada Medical, Oxford, UK) by one reader (COM) and reviewed with a second reader (UM) in consensus. For all lesions, SUVmax and SUVmean were recorded. A threshold of 41% of SUVmax was used to generate a contoured volume (mm^3). This threshold was used as it has been previously suggested to represent the optimal volume match (9). For reference, the SUVmax and SUVmean of the right parotid gland, liver (as measured over the right hepatic lobe) and mediastinal blood pool were recorded. Each lesion received a miPSMA score, prior to the below explained correction, as per the Prostate Cancer Molecular Imaging Standardized Evaluation (PROMISE) criteria.

Correction Methodology

For all analyses performed in this work, unsmoothed PET image data were used. Considering that the data utilized in this work was collated retrospectively from a cohort of patients undergoing PSMA PET as part of one of two ongoing clinical trials, post-

reconstruction smoothing was already applied to the images. The unsmoothed data were obtained by Richardson-Lucy deconvolution (10, 11). We validated this method within a subset of patients having available PET raw data, which were directly reconstructed without a smoothing filter for comparison.

CT and PET mask volumes were generated from the contours by selecting the pixels contained within the region contour points, slice-by-slice. To account for local alignment inconsistencies between PET and CT images, translational offsets for each individual lesion represented in the CT data were found which maximized the ROI peak SUV within the activity in the PET volume delineated by the corresponding region in the PET mask. The CT mask was then transformed to the PET space by linear interpolation onto the PET voxel coordinate grid, accounting for any necessary translational adjustments. Lesion volume and SUV data were recorded from the contoured lesions (“original dataset”).

The matched anatomical mask was the basis for calculating the PVC factors. However, prior to calculating the corrections factors, the relative contrast for each node needed to be represented in the mask, since local differences between region and background values determine partial volume spill-over effects. This was accomplished through an empirical searching approach; every region was scaled by a large range of contrast values, each time followed by the calculation of its respective partial volume correction map. The correction maps were then applied to the PET volumes and the resulting “corrected” activity distributions were summed over all affected voxels. The points of the sum data were fit to a curve, and the location on the curve which equaled the corresponding sum of the original data indicated that the total mass of activity had been preserved and hence yielded the correct scaling factor. The method outlined here

describes an approach for PVC for lymph nodes in PET images, with the assumption of uniformly distributed activity within small volumes.

Once each ROI in the mask was corrected and scaled appropriately against a unitary background, a map of the local PVC factors was generated. Partial volume effects were first simulated in the anatomical mask by filtering the volume by a 3D smoothing kernel consistent with the intrinsic scanner response function – in this experiment, a Gaussian kernel of 4 mm FWHM was used to model the point spread response. Dividing the original anatomical volume by the smoothed data yielded a map of correction factors which was then applied directly to the PET volume.

The effects of the PVC were evaluated for all regions in both unsmoothed and 5mm Gaussian post-smoothed images. The original versus corrected SUVmax and SUVmean were compared.

Subsequently, the prospectively assigned miPSMA score was compared to the score obtained from the corrected dataset [Figure 1]. All quantitative and qualitative assessment was correlated for lesion volume. Furthermore, a correction factor (CF) was calculated as follows: $[\text{SUVmax with PVC correction}] / [\text{original SUVmax}]$ for each lesion. In order to determine whether differences in pixel sizes from the two scanners play a significant impact in PVC method, the datasets were also analyzed separately for each scanner.

As in routine clinical work it is not practical to contour each node, the mean CF for lesions according to size groups was calculated. The size groups chosen were nodes > 9 mm in short axis (considered abnormal on morphological imaging); < 4mm (within range of scanner spatial resolution), and 2 categories for all lesions between 4 -9 mm (4-7mm and 7-9mm). This was done in order to generate a “rule of thumb” (RoT) CF according to

lesion size which could be used clinically. To validate this, the adjusted dataset using the mean CF per lesion size group was compared to the corrected SUV dataset. Similarly, the miPSMA scores were adjusted using unsmoothed reference tissues, and compared to the corrected dataset following the same methodology.

Statistical Analysis

Statistical analysis was performed using PAST software v.3.26. Paired student's t-test was used to compare lesion SUVmax before and after corrections for the entire cohort and for each lesion size group. PSMA scores before and after corrections were compared for each size group using Chi square test. A p -value of 0.05 or less was deemed statistically significant.

RESULTS

There were 142 men with biochemical recurrence of prostate cancer with negative CT and bone scintigraphy referred for ^{18}F -DCFPyL PET/CT. Of these, 67 patients were excluded from analysis due to negative PET [n=52]; lesions which could not be reliably contoured (details below) [n=13]; and indeterminate lung nodules [n=2]. The final study cohort consisted of 75 men with a median age of 69 years (range: 50 – 89) who were post radical prostatectomy [n=69], brachytherapy [n=5] or focal ablation therapy with high-intensity focused ultrasound (HIFU) [n=1]. Median serum PSA was 3.69 ug/L (range: 0.55 - 49.9).

Overall there were 271 suspected metastases on ^{18}F -DCFPyL PET/CT. Of them, 39 lesions were excluded due to inability to accurately contour on non-contrast CT (n=29) or PET (n=10). For example, bone lesions visualized on PET could not be contoured due to absence of morphological correlate on CT; or difficult delineation on PET for lesions adjacent to structures with high physiological PSMA activity such as ureter or bladder. The final cohort consisted of 232 well-defined nodal deposits (Siemens mCT [n=111]; GE Discovery 610 [n=121]).

Original vs Corrected Lesion Parameters

The mean lesion volume was $313.5 \pm 309.6 \text{ mm}^3$ [range, 15.3-1661]. Comparison of SUVmax, SUVmean and miPSMA score before and after correction is described in Table 2. The CF as a function of lesion volume as well as pixel size for the 2 different scanners used is displayed in Figures 2A & 2B. The mean CF by size group is provided in Table 3. The differences in original and corrected SUVmax and their corresponding miPSMA scores are presented as a function of lesion size in Tables 4 and Figure 3. The

corrected and RoT obtained SUVmax and miPSMA scores are shown in Table 5 and the distribution of miPSMA scores per lesion size for the various groups in Table 6.

Corrected vs RoT Lesion Parameters

The SUVmax and miPSMA scores obtained before and after correction method and using the “RoT” CF are presented in Table 3. Overall miPSMA scores were concordant between the corrected dataset and RoT in 205/232 lesions (88.4%). The level of concordance was moderate for small lesions and increased with lesion size (68.2% [15/22] for lesions < 4mm, increasing to 90.5% [190/210] for lesions greater than 4 mm in diameter).

DISCUSSION

The recently introduced PROMISE criteria are a standardized reporting framework for PSMA-ligand PET. Functional data from PET, including degree of tracer uptake compared to physiological uptake in reference tissues, are used in conjunction with morphological imaging data and clinical likelihood to derive a probability of malignancy. Local tumor extent, nodal metastases and distant metastases are assigned a molecular imaging TNM (miTNM) category. Although for regional nodes any PSMA uptake is considered positive for metastases, for nodes in less common locations for metastases, namely those outside of the abdomen or pelvis, the degree of PSMA uptake impacts interpretation. For example, a supraclavicular lymph node with miPSMA score of 1 would be considered negative; whereas if avidity is above liver uptake (miPSMA score of 2), the node would be considered positive for metastatic disease.

The role of PSMA PET in identifying patients with oligometastatic prostate cancer likely to benefit from metastases-directed ablative therapies is evolving. This therapeutic approach aims to obtain disease control by treating all molecularly-unveiled disease foci, thereby delaying or potentially avoiding the need for systemic therapies (12-14). PSMA PET is increasingly being used earlier during prostate cancer staging and re-staging, when conventional morphological imaging (e.g. CT and bone scintigraphy) are negative, highlighting the importance of these corrections for adequate characterization of subclinical small volume metastases.

In this work, we have shown that post-reconstruction smoothing and partial volume correction have a significant effect on quantitative and qualitative characterization of small nodal deposits. PSMA score may be sensitive to small variations in pixel SUV; therefore, quantitative accuracy is an important consideration for reliable and reproducible interpretation. The effect of image smoothing and partial volume on semiquantitative

uptake values of small lymph nodes on PSMA PET, as expressed by the calculated CF decreases exponentially with lesion size. As a result, the influence of this correction on the miPSMA score assigned to each lesion is greater for smaller lesions. For all lesions \leq 7 mm in diameter, a miPSMA score of 1 was assigned to 110/162 (68%) of lesions, compared to 36/162 (22.2%) after correction. Although there is a higher signal recovery for small lesions with smaller pixel size (Figure 2A), overall the trend was similar for both pixel size images evaluated in this study.

These correction methods are time consuming and technically challenging, and impractical for routine adoption in clinical practice. Nonetheless, quantitative accuracy is becoming increasingly important in precision cancer imaging, for clinical diagnosis, improving consistency across multicenter clinical trials, and for therapy planning and delivery (15). As such, we suggest the use of a simplified, empiric approach for correction of PSMA uptake by applying a specific RoT CF for small lesions according to their size category. This could be easily applied clinically when using the PROMISE diagnostic algorithm for small PSMA-avid nodes. Overall there is good concordance of the miPSMA score obtained using the RoT with the corrected miPSMA score (nearly 90%). Furthermore, the impact of the discordance between miPSMA scores obtained using correction methods versus the RoT on clinical interpretation is likely minor when considering that for many of these lesions (e.g. nonregional nodes or indeterminate bone lesions on CT) a score of 2 is sufficient for diagnosis of a metastatic deposit, and a discordance between score of 2 and 3 is unlikely to be clinically relevant.

This study has several limitations. First, the patient cohort is a selected population of patients with biochemical failure in whom CT and bone scintigraphy are negative or equivocal. Therefore, these corrections in patients with higher volume metastatic disease would likely be less clinically relevant. Second, we only included lymph nodes in our

analyses. None of the bone lesions encountered had a CT correlate, therefore could not be segmented accurately for the correction methods used, and none of the patients had proven visceral metastases on PET. It is conceivable that the CF identified for nodes may not be applicable for all metastatic sites. Third, the use of 2 different scanners introduces heterogeneity to the data; however, we analyzed the data separately for each scanner according to pixel size. Fourth, the impact of PVC on regional nodal metastases is unlikely to be clinically relevant, as regional nodes with a score of 1 are considered positive; however, this could impact the classification of other deposits such as non-regional nodes. Fifth, we did not have pathology confirmation of PSMA avid nodes. Finally, this study used a second generation ^{18}F -labelled PSMA-ligand and it is uncertain whether these results can be extrapolated to ^{68}Ga -PSMA tracers, or to other ^{18}F -labelled tracers with different biodistribution and different background tracer uptake at reference tissues.

In conclusion, there is a significant effect of smooth filter and partial volume correction on measured PSMA activity in small nodal metastases, impacting the miPSMA score. We propose the use of a simplified, clinically applicable RoT CF for tracer uptake in small lesions. The impact of these changes on the management and outcomes of patients with oligometastatic prostate cancer need validation in future clinical studies.

KEY POINTS

Question: Do partial volume effect and post-processing smoothing of images significantly impact the measured PSMA activity in small prostate cancer metastases and does this influence the miPSMA score?

Pertinent Findings: In this prospective cohort study, there is a significant effect of smooth filter and partial volume correction on measured PSMA activity in small nodal metastases, impacting the miPSMA score.

Implications for Patient Care: When evaluating PSMA PET, a correction for partial volume effect and smoothing needs to be applied for small metastatic lymph nodes.

REFERENCES

1. Hope TA, Afshar-Oromieh A, Eiberr M, et al. Imaging prostate cancer with PSMA PET/CT and PET/MR: current and future applications. *AJR Am J Roentgenol.* 2018;211(2):286-294.
2. Werner RA, Derlin R, Lapa C, et al. ¹⁸F-Labeled, PSMA-Targeted Radiotracers: Leveraging the Advantages of Radiofluorination for Prostate Cancer Molecular Imaging. *Theranostics.* 2020;10(1):1-16.
3. Szabo Z, Mena E, Rowe SP, et al. Initial evaluation of [¹⁸F]DCFPyL for Prostate-Specific Membrane Antigen (PSMA)-Targeted PET imaging of prostate cancer. *Mol Imaging Biol.* 2015;17(4):565-574.
4. Eiber M, Herrmann K, Calais J, et al. Prostate Cancer Molecular Imaging Standardized Evaluation (PROMISE): proposed miTNM classification for the interpretation of PSMA-ligand PET/CT. *J Nucl Med.* 2018;59:469-478.
5. Soret M, Bacharach SL, Buvat I., et al. Partial-volume effect in PET tumor imaging. *J Nucl Med.* 2007;48:932-945.
6. Boussion N, Cheze Le Rest C, Hatt M, Visvikis D, et al. Incorporation of wavelet-based denoising in iterative deconvolution for partial volume correction in whole-body PET imaging. *Eur J Nucl Med Mol Imaging.* 2009;36:1064-1075.
7. Cysouw MCF, Kramer GM, Schoonmade LJ, et al. Impact of partial-volume correction in oncological PET studies: a systematic review and meta-analysis. *Eur J Nucl Med Mol Imaging.* 2017;44:2105-2116.
8. Ravert HT, Holt DP, Chen Y, et al. An improved synthesis of the radiolabeled prostate-specific membrane antigen inhibitor, [¹⁸F]DCFPyL. *J Labelled Comp Radiopharm.* 2016;59:439-450.

9. Biehl K, Dehdashti F, Feng Ming K et al. 18F-FDG PET definition of gross tumor volume for radiotherapy of non-small cell lung cancer: Is a single standardized uptake value threshold approach appropriate? *J Nucl Med.* 2006;47(11):1808-1812.
10. Lucy LB. An iteration technique for the rectification of observed distributions. *Astron J.* 1974;79:745-754.
11. Richardson WH. Bayesian-based iterative method of image restoration. *J Opt Soc Am.* 1972;62(1):55-59.
12. Ost P, Reynders D, Decaestecker K, et al. Surveillance or metastases-directed therapy for oligometastatic prostate cancer recurrence: A prospective, randomized, multicenter phase II trial. *J Clin Oncol.* 2018;36:446-453.
13. Tosoian JJ, Gorin MA, Ross AE, et al. Oligometastatic prostate cancer: Definitions, clinical outcomes, and treatment considerations. *Nat Rev Urol.* 2017;14:15-25.
14. Kneebone A, Hruby G, Ainsworth H, et al. Stereotactic body radiotherapy for oligometastatic prostate cancer detected via prostate-specific membrane antigen positron emission tomography. *Eur Urol Oncol.* 2018;1:531-537.
15. Wright CL, Binzel K, Zhang J, Knopp MV. Advanced functional tumor imaging and precision nuclear medicine enabled by digital PET technologies. *Contrast Media Mol Imaging.* 2017:5260305.

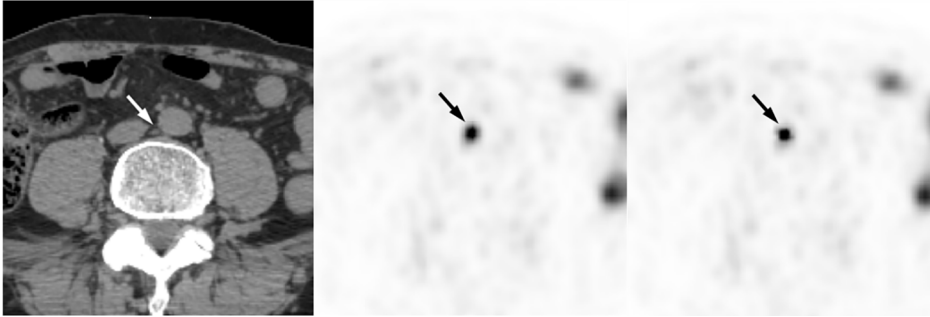


Figure 1. 75 year old man with history of pT3a Gleason 7 (3+4) prostate cancer post radical prostatectomy 11 years ago, and salvage radiotherapy for biochemical recurrence 7 years ago. Now slowly rising PSA (2.1 ng/mL).

Inter-aortocaval lymph node (left white arrow) with volume of 118.3 ml³ on CT (left). SUVmax measured on PET was 7.0 with a miPSMA score of 1 (middle black arrow). After correction, SUVmax was 22.6 with a miPSMA score of 3 (right black arrow).

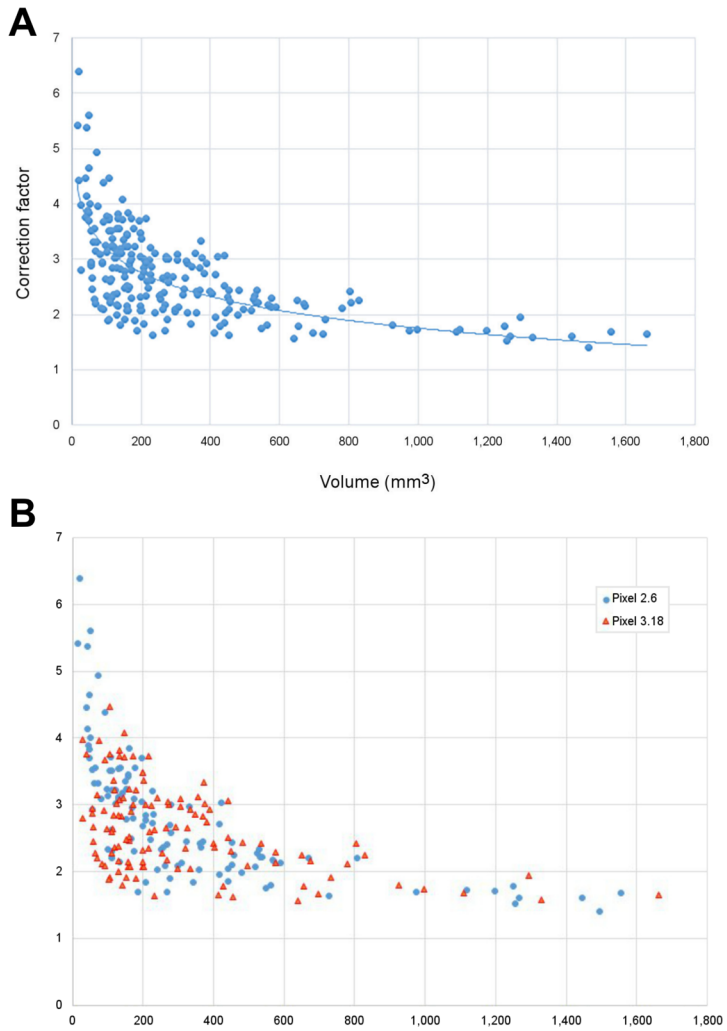


Figure 2. Correction factor as per lesion volume

- a. Distribution of correction factors (y-axis) by lesion volume in mm³ (x-axis)
- b. Correction factor by volume and pixel size (red triangle 3.18 mm; blue circle 2.6 mm)

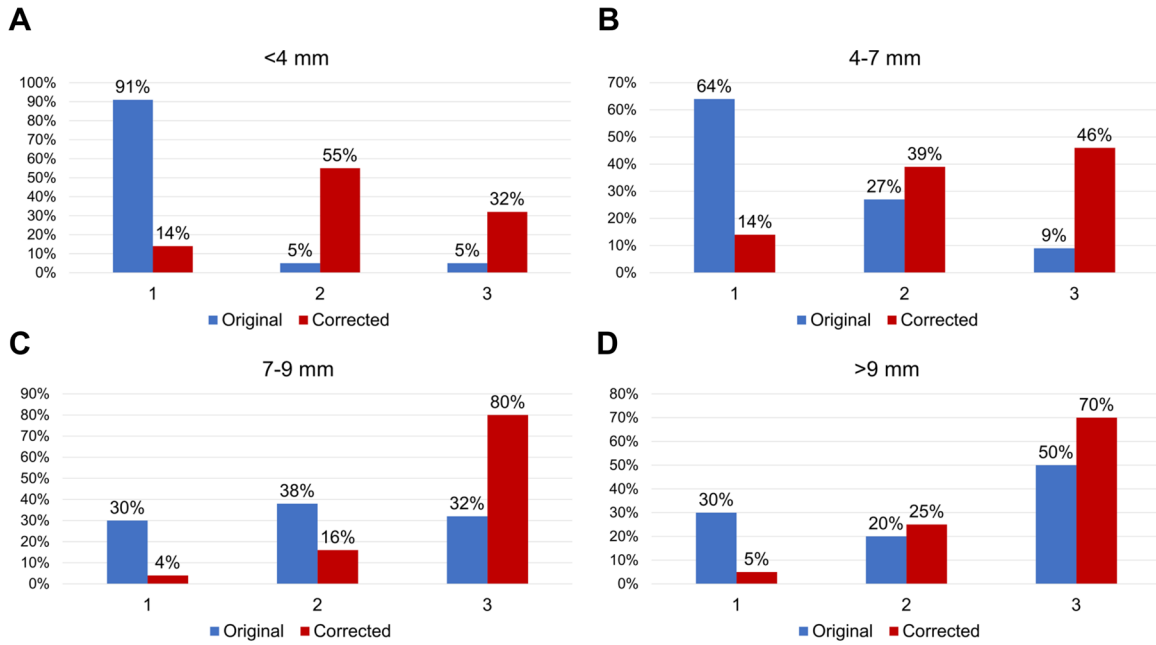


Figure 3. Distribution of PSMA scores as a function of lesion size before and after smooth filter and partial volume correction.

- a. For lesions below 4 mm
- b. For lesions between 4 and 7 mm
- c. For lesions between 7 and 9 mm
- d. For lesions between 9 and 12 mm

TABLES

Score	PSMA expression	Uptake
0	No	Below blood pool activity
1	Low	≥ Blood pool & < Liver
2	Intermediate	≥Liver & < Parotid gland
3	High	≥ Parotid gland

Table 1. PSMA scoring system

	Original Values	Corrected Values
	± SD	± SD
	[range]	[range]
Mean SUVmax *	11.0 ± 9.3 [1.8-57.1]	28.5 ± 22.8 [5.1-116.3]
Mean SUVmean *	6.7 ± 5.7 [1-36.3]	14.1 ± 11.3 [2.2-54.8]
Mean miPSMA score †	1.6 ± 0.76 [1-3]	2.28 ± 0.77 [1-3]

Table 2. Original vs corrected parameters for all lesions

SD = standard deviation;

* $p < 0.00001$;

† $p < 0.00001$

Lesion size (n=)	Correction Factor Mean (range ± SD)
< 4 mm (n=22)	4 (2.5-6.4 ± 1.1)
4-7 mm (n=140)	2.8 (1.6-4.9 ± 0.64)
7-9 mm (n=50)	2.3 (1.6-3.3 ± 0.43)
9-12 mm (n=20)	1.8 (1.4-2.4 ± 0.64)

Table 3. Correction Factor as per Lesion Size.

SD = Standard Deviation

	Original values		Corrected values	
	<i>SUVmax</i> ± SD [range]	<i>miPSMA</i>	<i>SUVmax</i> ± SD [range] <i>p</i> -value*	<i>miPSMA</i> ± SD <i>p</i> -value†
<4 mm	5.3 ± 5.2 [2.1-25.6]	1.1 ± 0.5	21.5 ± 21.2 [5.6-96.3] <i>p</i> =0.00072*	2.1 ± 0.8 <i>p</i> <0.00001†
4-7 mm	8.4 ± 6.0 [1.8-34.3]	1.4 ± 0.6	24.4 ± 19.7 [5.1-116.3] <i>p</i> <0.00001*	2.2 ± 0.8 <i>p</i> <0.00001†
7-9 mm	16.4 ± 9.2 [3.7-45.8]	2.0 ± 0.8	39.0 ± 25.5 [5.8-102.9] <i>p</i> <0.00001*	2.6 ± 0.7 <i>p</i> <0.00001†
9-12 mm	22.2 ± 15.6 [3.8-57.1]	2.2 ± 0.9	39.2 ± 27.1 [8.4-102.0] <i>p</i> =0.00004*	2.5 ± 0.8 <i>p</i> =0.114†

Table 4. Original vs Corrected SUVmax & miPSMA scores

SD= standard deviation

* *p* values obtained comparing original vs corrected SUVmax

† *p* values obtained comparing original miPSMA score vs corrected miPSMA

	Corrected values		RoT* values	
	<i>SUVmax</i> ± SD [range]	<i>miPSMA</i> *	<i>SUVmax</i> ± SD [range] <i>p</i> -value †	<i>miPSMA</i> <i>p</i> -value ‡
<4 mm	21.5 ± 21.2 [5.6-96.3]	2.1 ± 0.8	21.0 ± 20.4 [8.3-101.4] <i>p</i> =0.681†	2.1 ± 0.6 <i>p</i> =0.616‡
4-7 mm	24.4 ± 19.7 [5.1-116.3]	2.2 ± 0.8	23.7 ± 16.8 [5.1-96.7] <i>p</i> =0.184†	2.3 ± 0.8 <i>p</i> =0.665‡
7-9 mm	39.0 ± 25.5 [5.8-102.9]	2.6 ± 0.7	37.4 ± 21.0 [8.4-104.5] <i>p</i> =0.206†	2.6 ± 0.7 <i>p</i> =0.905‡
9-12 mm	39.2 ± 27.1 [8.4-102.0]	2.5 ± 0.8	40.1 ± 28.1 [6.9-103.0] <i>p</i> =0.595†	2.5 ± 0.8 <i>p</i> =0.867‡

Table 5. Corrected versus “Rule of thumb” SUVmax & miPSMA scores

SD= standard deviation

* RoT = values obtained applying “rule of thumb” correction factor to the original dataset

† *p* values obtained comparing original vs corrected SUVmax

‡ *p* values obtained comparing original miPSMA score vs miPSMA obtained after correction

	Original			Corrected			RoT *		
	n= (%)			n= (%)			n= (%)		
miPSMA score	1	2	3	1	2	3	1	2	3
<4 mm	20 (91)	1 (4.5)	1 (4.5)	5 (22.7)	10 (45.5)	7 (31.8)	3 (13.6)	13 (59.1)	6 (27.3)
4-7 mm	90 (64.3)	38 (27.1)	12 (8.6)	31 (22.1)	51 (36.4)	58 (41.4)	25 (17.9)	53 (37.8)	62 (44.3)
7-9 mm	15 (30)	19 (38)	16 (32)	6 (12)	10 (20)	34 (68)	5 (10)	9 (18)	36 (76)
9-12 mm	6 (30)	4 (20)	10 (50)	4 (20)	3 (15)	13 (65)	3 (10)	4 (25)	13 (65)

Table 6. Distribution of original, corrected and RoT miPSMA scores.

* RoT = values obtained applying “rule of thumb” correction factor to the original dataset